LIMNOLOGY and OCEANOGRAPHY

ASLO

Limnol. Oceanogr. 9999, 2021, 1–17

doi: 10.1002/lno.11891

Eavesdropping on plankton—can zooplankton monitoring improve forecasting of biotoxins from harmful algae blooms?

Aubrey Trapp [1,3*] **Jan Heuschele** [2] **Erik Selander** [1]

[1]Department of Marine Sciences, University of Gothenburg, Gothenburg, Sweden
[2]Section for Aquatic Biology and Toxicology, Department of Biosciences, University of Oslo, Oslo, Norway
[3]Present address: Department of Ocean Sciences, University of California Santa Cruz, Santa Cruz, California

Abstract

Harmful algae bloom (HAB) forecasting has developed rapidly over recent decades, but predicting harmful levels of marine biotoxins in shellfish is still a challenge. New discoveries suggest that predator-prey interactions may be an important driver in the formation of HABs. Key species of harmful algae respond to copepod infochemicals with increased toxin production. In addition, copepods feed selectively on less defended prey, which may further promote harmful taxa. Here we explore if eavesdropping on predator-prey dynamics by monitoring zooplankton can improve HAB forecasting. We first examine an 8-yr time series including copepod biomass, harmful algae cells (*Dinophysis* spp.), and diarrhetic shellfish toxins in blue mussels (*Mytilus edulis*) using generalized additive models. Models including copepod biomass more accurately predicted okadaic acid in mussels than phytoplankton alone. We then apply this connection more narrowly by analyzing the specific copepod exudates known to induce toxin production, copepodamides, from the mussels sampled in biotoxin monitoring. Adding copepodamide data from shellfish extracts increased model performance compared to copepod biomass. Results suggest that including grazing effects through copepodamide measurements may provide a cost-efficient way to improve accuracy and lead time for predicting the accumulation of microalgal toxins in shellfish.

Harmful algae blooms (HABs) are a global challenge for aquaculture and local shellfish consumers. The need for accurate forecasting has driven rapid technical development including molecular tools (Humbert et al. 2010), remote sensing (Zhang et al. 2013; Anderson et al. 2016), and chemical identification of novel toxic compounds (Suzuki et al. 2012; Tillmann et al. 2017). Advances in uptake kinetics have strengthened our understanding of the link between HABs and the accumulation of toxins in shellfish (Blanco 2018). In situ imaging and molecular sensors are increasing the amount of available data for aquatic ecosystems, and automatic identification of harmful taxa by deep learning algorithms shows great potential (Grasso et al. 2019; Hill et al. 2020; Spanbauer et al. 2020). Remaining hurdles to predictive monitoring include high intraspecific variation in toxin profile and content and the costs (Seltenrich 2014). Consequently, manual phytoplankton cell counts and biotoxin analyses in shellfish are still vital components of HAB control (Naustvoll et al. 2012; Davidson et al. 2016; O'Mahony 2018). The relationship between phytoplankton abundance and toxin accumulation in shellfish is highly variable, and cell counts are generally unreliable for more than a few days of early warning (Dahl and Johannessen 2001; MacKenzie et al. 2004).

Collaborative efforts working to develop a global HABs observing network support improving current cost-effective forecasting systems and merging new ecological models with existing Earth systems models (Anderson et al. 2019). Grazing effects are rarely included in forecasting models, though top-down pressure from grazers is known to influence HAB variability (Turner and Tester 1997; Smayda 2008; Hong et al. 2013). Two potentially important mechanisms behind these predator-prey interactions are grazer avoidance of harmful taxa and the induction of chemical defenses. Rejection or avoidance by grazers may increase the relative abundance of harmful taxa when grazers are present in high densities (Teegarden et al. 2001; Prevett et al. 2019). In addition, harmful species of dinoflagellates (*Alexandrium* spp.), diatoms (*Pseudo-nitzschia* spp.), and cyanophyceans (*Microcystis*

*Correspondence: ajtrapp@ucsc.edu

Additional Supporting Information may be found in the online version of this article.

aeruginosa) increase toxin production in response to grazer presence (Jang et al. 2003; Senft-Batoh et al. 2015; Selander et al. 2019). Grazer-induced toxin production may enhance the feeding preferences of grazers and further increase the proportion of harmful algae that contribute to biotoxin accumulation in shellfish and other marine animals.

Copepods grazing on the phytoplankton community exude a unique bouquet of polar lipids, collectively known as copepodamides. Copepodamide concentrations in seawater correlate with copepod density (Selander et al. 2015, 2019). In response to copepodamides, diverse taxa express defensive traits, including toxin production, increased bioluminescence, colony size plasticity, and decreased cell size (Selander et al. 2015; Lindström et al. 2017; Prevett et al. 2019). Moreover, these cues trigger toxin production in both dinoflagellates (*Alexandrium* spp.) and diatoms (*Pseudo-nitzschia* spp.) at ecologically relevant concentrations (Selander et al. 2015, 2019). Figure 1 illustrates a potential response pathway from exudation of copepodamides by copepods to toxin accumulation in mussels. Upregulation of defensive traits and selective grazing by copepods are well established in simplified laboratory settings (Teegarden et al. 2001; Selander et al. 2006). Prevett et al. (2019) indicates these mechanisms lead to increased relative abundance of the defended phenotype in nature too, but the extent this contributes to harmful algal blooms and toxin content in mussels has yet to be tested. We hypothesize that accumulation of copepodamides by mussels will precede the proliferation of toxic dinoflagellates and the eventual accumulation of microalgal toxins by mussels.

Here we focus on a practical application of this predator-prey interaction and explore if the past history of grazer abundance and grazer cues can improve forecasting of biotoxins in blue mussels. First, we test the relationship between copepod density and the most frequently occurring taxa of harmful algae in the area (*Dinophysis* spp.) with corresponding shellfish toxins, okadaic acid (OA), DTX-1, and DTX-2, in generalized additive models constructed from 8 yr of monitoring data. Second, we show that copepodamides accumulate in mussels and estimate the degradation rate. Finally, we measure copepodamides in mussel samples weekly over 9 months to investigate the predictive correlation observed in the long-term monitoring study at greater spatial and temporal resolution. Measuring copepodamides from the same mussel samples that are tested for toxins gives location accurate data in a cost-efficient way. For example, labs that already measure biotoxins by mass spectrometry may be able to integrate zooplankton information by adding a copepodamide analysis to routine lipophilic biotoxin samples using the same instrumentation. Additionally, a global shift toward toxin quantification by chemical analysis has proved safer and more effective than the traditional mouse bioassay for both diarrhetic and paralytic toxins (Turrell and Stobo 2007; Turner et al. 2011, 2012), which suggests increased access to instrumentation for monitoring copepodamides in the future.

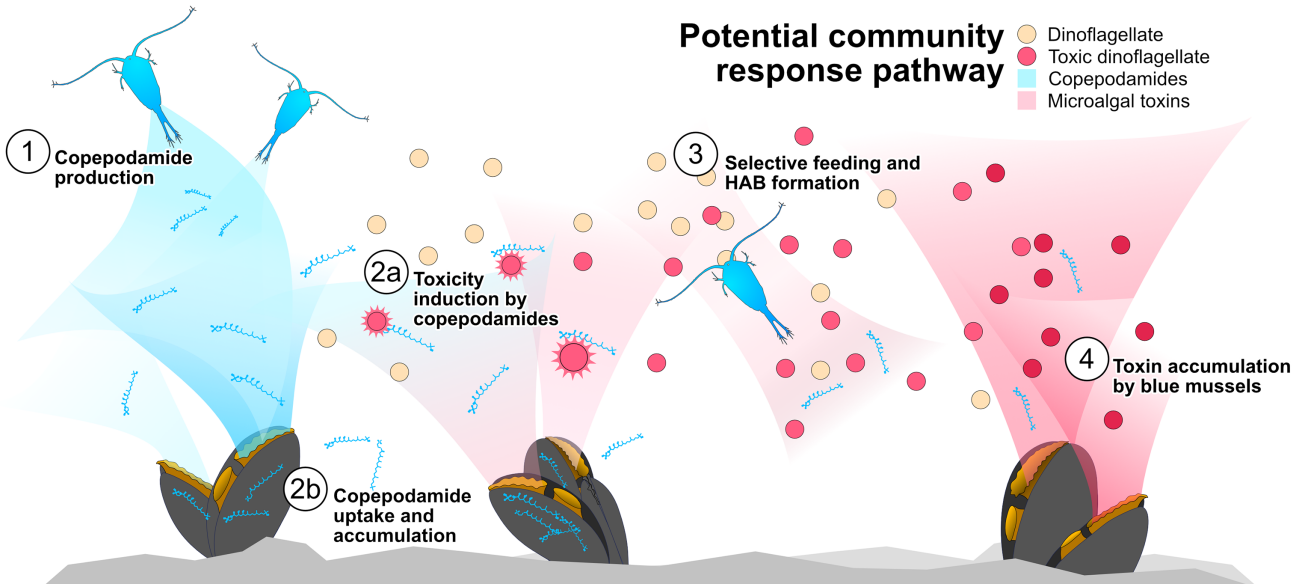

Fig. 1. Hypothesized community response pathway from copepodamide production to the accumulation of biotoxins in mussels. (1) Copepods exude copepodamides to the surrounding water (Selander et al. 2019). (2a) Copepodamides trigger increased toxin production in some harmful taxa (Selander et al. 2015, 2019), and (2b) accumulate in filter feeding bivalves (present study). (3) Copepods feed selectively on less toxic prey items, thereby increasing the relative abundance of the harmful taxa (Teegarden et al. 2001; Xu and Kiørboe 2018). (4) Mussels accumulate toxins while feeding on a community with larger proportion of harmful taxa and grazer-induced cell-specific toxin content. Contributions from copepods and toxic dinoflagellates are indicated by blue and red, respectively.

Methods

Plankton monitoring data acquisition for biotoxin models

Copepod abundance was retrieved from the public database, SHARKweb, maintained by the Swedish Meteorological and Hydrological Institute (SMHI). The copepod data set includes measurements from two stations on the Swedish West Coast between October 2011 and December 2018 (Fig. 2). While there are four total stations that monitor copepods on the Swedish West Coast, only two stations were centered in the region where harmful algae and toxins are also measured. Copepods from the 11 most abundant genera (*Temora*, *Calanus*, *Oithona*, *Paracalanus*, *Microsetella*, *Clausocalanus*, *Metridia*, *Centropages*, *Microcalanus*, *Pseudocalanus*, and *Acartia*) and six stages (Copepodite 1–5 and adults) were included. A single data point (22 November 2013) was four orders of magnitude higher than all other data and was excluded from the analysis. Copepod abundance measurements were converted to biomass using the formula and coefficients compiled in Bjærke et al. (2015). All genera and life stages were summed to give a total copepod biomass for each sampling location on each sampling date and interpolated to give weekly resolution.

Biotoxin data were generously provided by the shellfish monitoring program at the Swedish Food Agency. Toxin measurements were included from 25 sites on the Swedish West Coast between September 2010 and January 2019 (Fig. 2). Only data from *M. edulis* samples were included. Diarrhetic shellfish toxins (DSTs) from the OA group were monitored separately as OA, DTX-1, and DTX-2, and as a combined measurement called DST-total (Sundh and Toljander 2017). One DST measurement from Halsefjorden in 2013 was recorded lower than the reported threshold of the analysis (30 μg OA eq kg^{-1} mussel), so it was believed to be a reporting error and removed. Toxin concentration for each parameter was averaged across stations to produce a conservative mean for each sampling date and then across all dates per week.

Phytoplankton data were also retrieved from the public database, SHARKweb, maintained by SMHI. Phytoplankton measurements included 24 stations on the Swedish West Coast between January 2010 and December 2018 (Fig. 2). Abundance data for *Dinophysis acuminata*, *Dinophysis acuta*, and *Dinophysis norvegica* were summed for each station on each sampling date. Weekly means across all stations were calculated for the study period.

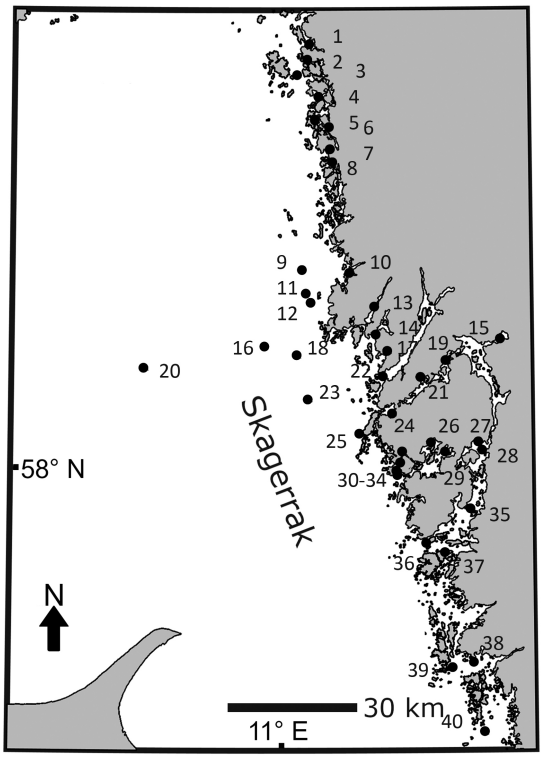

No	Station	Copepodamides	Toxins	Copepods	Dinophysis
1	Strömstadsfjorden		3		
2	Tjärnöarchipelago	22	108		
3	Kosterfjorden				195
4	Råssö-Resöfjorden		2		
5	Lindöfjord		36		
6	Sannäsfjorden		6		62
7	Fjällbacka		1		150
8	Sövall		1		
9	Stridsfjorden		1		
10	Bottnafjorden	20	204		166
11	Edsvik		1		
12	Grebbestad		2		
13	Åbyfjorden	15	164		
14	Strettuden				228
15	Byfjorden				15
16	Å13				63
17	Saltöfjorden		153		311
18	OK001				28
19	Kalvöfjorden	2	70		
20	Å17			64	105
21	Borgilefjord		141		2
22	Släggö			81	391
23	Byttelocket				56
24	Havstensfjorden	31	506		370
25	Koljöfjorden	1	219		206
26	Ljungskile	9	276		
27	Halsefjorden		262		
28	Galterö				86
29	Stigfjorden	30	402		
30	Lyresund	8	290		418
31	Tångesund				22
32	Boxvikskile	1	164		
33	Kråkefjorden		145		
34	Käringöfjorden		6		
35	Hakefjorden		1		24
36	Åstol				233
37	Instö Ränna				81
38	Skalkgorna				75
39	Danafjord				232
40	Valö				27
Number of samples		**139**	**3164**	**145**	**3546**

Fig. 2. Sampling stations for copepods, copepodamides, phytoplankton, and toxins. Station locations and sampling frequency for toxins, copepods, and phytoplankton were determined by monitoring programs at the Swedish Food Agency and Swedish Meteorological and Hydrological Institute (SMHI). The two monitoring stations for zooplankton (20 and 22) are located in the center of the study area. Copepodamides were measured from mussels at the most frequently sampled toxin stations during 2018.

For the long-term analysis, including 8-yr of monitoring data, copepods were sampled by the monitoring agency with lower temporal and spatial resolution than the other parameters, approximately monthly from two stations. Monitoring related to HABs was more frequent, and both toxins and phytoplankton were sampled weekly. We addressed the unbalanced sample frequencies by linearly interpolating for each missing day between existing data points and calculating weekly means for each parameter. We also include an analysis with copepodamides that avoids the sparse copepod data set, because copepodamides and toxins were analyzed from the same weekly samples. Monitoring data for copepods, toxins, and phytoplankton can be found in Supporting Information Appendix S1.

The short-term analysis, which includes copepodamides, spanned 8 months from May to December, 2018. In this subset of data from the long-term analysis, there were 156 *Dinophysis* samples with counts recorded weekly from five stations throughout the study area. There were also 263 mussel samples analyzed for DST-total, which includes both DTX and OA. Mussel samples were collected weekly from seven stations. We also took 139 copepodamide measurements, which were recorded weekly from 10 stations. Sta. 2, 10, 13, 24, and 29 were sampled most frequently, but mussel samples from other sites were included as necessary to make up at least three copepodamide measurements per week (Fig. 2).

Copepodamide extraction and analysis for biotoxin models

Homogenized *M. edulis* soft tissue samples were received from the Swedish Food Agency. Mussel homogenate was aliquoted into a 24-well plate, frozen overnight (−20°C), and freeze-dried (Chaist LMC-1 dryer, Pfeiffer Duo 10 pump) for 22 h. Dry homogenate (400 mg) was extracted in 4 mL methanol for 24 h and centrifuged (Jouan SA Centrifuge CR213, France) at 2500 rpm for 10 min. Supernatant was transferred to a clean glass tube. Mussel extracts were dried under a stream of N_2, resolved in 1.5 mL methanol, and transferred to liquid chromatography vials for analysis.

Copepodamide concentrations were determined by multiple reaction monitoring experiments on a triple quadrupole mass spectrometer (Agilent 6410). Briefly, a gradient elution of A: 35 : 35 : 30 methanol : acetonitrile : MilliQ water with 0.1% formic acid and B: 2-propanol with 0.2% formic acid was used to separate compounds. Copepodamides were identified and quantified against authentic standards by comparing retention time and presence of diagnostic fragments m/z 430 for copepodamides, and 432 for di-hydro copepodamides as in Selander et al. (2015). The structure-based nomenclature system for classifying copepodamides is described in Grebner et al. (2019). Diagnostic copepodamide fragments are collectively referred to as lyso-copepodamides. Copepodamide data and calculations can be found in Supporting Information Appendix S2.

Copepodamide accumulation in mussels

To test if blue mussels accumulate copepodamides from seawater, we performed simple accumulation and depuration experiments with copepodamides extracted from industrially fished *Calanus finmarchicus* (Calanus AS, Norway). *C. finmarchicus* is one of the dominating copepod species in the study area.

Blue mussels (*Mytilus edulis* Linnaeus, 1758) of average length 3.2 ± 0.5 cm were collected from a dock at the Sven Lovén Center at Tjärnö on 14 December 2018. The mussels were kept in running seawater until 20 January 2019. A total of 36 mussels were randomly allocated between six glass jars (3.3 L) with 2 L filtered seawater (salinity = 33, 15°C) and air bubbling. After acclimating for 30 min, three mussels were removed from each jar and frozen. Copepodamide dissolved in methanol was added to three jars to a final concentration of 1 nmol L^{-1}. An equal volume of methanol was added to three jars for control. Mussels were fed with *Rhodomonas salina* (GU Marine Culture—GUMACC, Gothenburg University, Sweden) to stimulate filter feeding. After 12 h, the remaining three mussels from each jar were removed and frozen.

Frozen mussels were cracked and freeze-dried for 22 h. The samples were weighed, homogenized, and extracted in 9 mL methanol for 24 h at room temperature. The extract was centrifuged at 2000 rpm for 10 min. Supernatant was dried under a stream of N_2, resolved in 150 μL methanol, and centrifuged again before transfer to a liquid chromatography vial with low volume insert.

The concentration of copepodamides in the mussel water was determined at the start of the experiment and after 12 h. Fifty milliliters of water was slowly drawn onto an SPE column (ABN, 100 mg, 3 mL reservoir, Biotage) that had been preconditioned with one column volume of methanol followed by one column volume MilliQ water. The column was desalted with one column volume MilliQ H_2O and copepodamides eluted in 3 mL methanol. The eluate was evaporated under a stream of N_2, resolved in 150 μL methanol, and stored frozen until analysis.

Copepodamide depuration in mussels

Blue mussels (*Mytilus edulis* Linnaeus, 1758, n = 54) of an average length 2.7 ± 0.4 cm were collected from the Sven Lovén Center at Tjärnö on 02 November 2018 and stored in running seawater for 36 h. They were randomly distributed into three glass jars (3.3 L) with 3 L of filtered, aerated seawater (salinity = 33, temperature = 15°C). Three mussels were removed from each jar and frozen at six time points (0, 12, 24, 48, 72, and 96 h). The mussels were fed three times per day with *R. salina* (100 cells mL^{-1}, GU Marine Culture—GUMACC, Gothenburg University, Sweden).

Mussels were cracked and freeze-dried for 22 h (Chaist LMC-1 dryer coupled to a Pfeiffer Duo 10 vacuum pump). One sample was composed of three individual mussels. The dried samples were weighed, homogenized, and extracted in 40 mL methanol. After 24 h, samples were centrifuged at

2500 rpm for 10 min (Jouan SA Centrifuge CR213, France) and supernatant was added to a clean tube. Extracts were dried under a stream of N_2, resolved in 1.5 mL methanol, and transferred to a liquid chromatography vial for chemical analysis as described above.

Statistics and analysis

The depuration of copepodamides in mussels over time was tested with a single factor ANOVA. Accumulation experiments were tested with a two-way ANOVA with the factors time and treatment. Levene's test was used to test for heterogeneous variances. The half-life of copepodamides was determined from least square linear curve fits to ln-transformed data. Experimental data and calculations can be found in the Supporting Information Appendix S3.

We used the long-term data set to test whether the detection of a toxin can be predicted using copepod and dinoflagellate data. We formulated generalized additive models with toxin detection (> 30 μg OA eq kg^{-1}) and absence (< 30 μg OA eq kg^{-1}) as a binomial response variable. We also used generalized additive models (gam, mgcv-package; Wood 2011) to assess whether copepod abundance data can predict the toxin concentration in mussels. In these models, two smooth functions of copepod biomass ($\mu g\ L^{-1}$) and dinoflagellate cell counts were the independent factors. Both model approaches were applied to toxins: DST-total, OA, and DTX-2.

Toxin concentrations below the detection limit of 30 μg OA eq kg^{-1} mussel were replaced with random numbers between 0 and 30 to reduce skewness prior to taking the weekly average. To ensure that this did not influence our model predictions, we repeated each previously described model 10 times and report the average model coefficients. Repeating the randomization and modeling procedure also gave us the opportunity to test the robustness of the model predictions.

To test whether copepodamide and dinoflagellate data correlate with concentration of DST-total and OA in blue mussels, we specified general additive models (gam, mgcv-package; Wood 2011) with the respective toxin as the dependent factor and two independent smooth functions for copepodamide concentration and dinoflagellate cell count as independent factors. To test if the inclusion of copepodamide data added explanatory power to the models, we also formulated a similar gam-model with a single smooth function for dinoflagellate cell counts as an independent factor.

All variables were ln-transformed to reduce positive skew. We used restricted maximum likelihood for parameter estimation and the inbuilt model selection feature of mgcv, which allows us to remove terms during the fitting process. Model parameterization, fit, and choice were examined using the gam.check function of the mgcv-package and by visually inspecting the distribution of the residuals in the resulting diagnostic plots. Analysis was done in R (version 3.6.1, R Core Team 2019).

The time from phytoplankton observations to toxin increase in shellfish ranges from 2 to 10 d (Godhe et al. 2002; Lindegarth et al. 2009; Swan et al. 2018). We therefore estimated that, on average, toxins will be detected in shellfish 1 week after an increase in phytoplankton abundance. The timescale of community response to copepods, including selective grazing and toxin induction, is more complex (Fig. 1). Grazer-induced toxin production typically requires 2–3 cell divisions (Selander et al. 2012), and the effect of selective grazing will be slow or absent when grazing pressure is low and high when grazing is intense. As a consequence, we estimated a community response of 4 weeks, and we explored results within a 9-week window of lead time.

Results

Modeling biotoxin with plankton monitoring data

Time series of copepod biomass, *Dinophysis* spp. abundance, and toxin content in blue mussels from the Swedish West Coast shows a seasonal pattern (Fig. 3). On average, 2011 had the highest DST concentrations in mussels and 2013 had the lowest. Copepod monitoring data shows an annual biomass high corresponding to the warm season. *Dinophysis* abundance peaks one to two times per year, and 2015 had the longest sustained *Dinophysis* bloom. Corresponding peaks across all parameters are most visible in late 2011 and 2015. Notably, in 2013 and to a lesser extent 2014 and 2017, *Dinophysis* abundance did not translate to high toxin content in mussels.

DSTs generally pose the greatest risk to aquaculture in the period from October to December (Rehnstam-Holm and Hernroth 2005), but monitoring data shows that DST measurements could exceed EU safety limits of 160 μg OA eq kg^{-1} in nearly every month of the year (Fig. 4). Separate analysis of OA and DTX-2 help to elucidate the DST-total pattern observed in Fig. 3. No samples were found to contain DTX-1. DTX-2 was a strong contributor to the DST-total concentration in blue mussels in 2011 and 2012, and OA was more prevalent in 2015 and 2018. OA was also more variable with toxin concentrations surpassing the safety threshold at different times of the year through the study period. In contrast, DTX-2 was most prevalent in the late fall and nearly undetectable in the summer for most years.

The data from the time series in Fig. 3 were used to model biotoxins in mussels with and without the inclusion of copepod biomass. The analysis shows the expected 1-week lead time for *Dinophysis* preceding increased toxin content in mussels. When we used copepod biomass with the originally hypothesized 4-week lead time, we detected a significant correlation between copepods and the presence of OA but not DST-total or DTX-2. A lead time of 7 weeks increased the explanatory power of copepods in

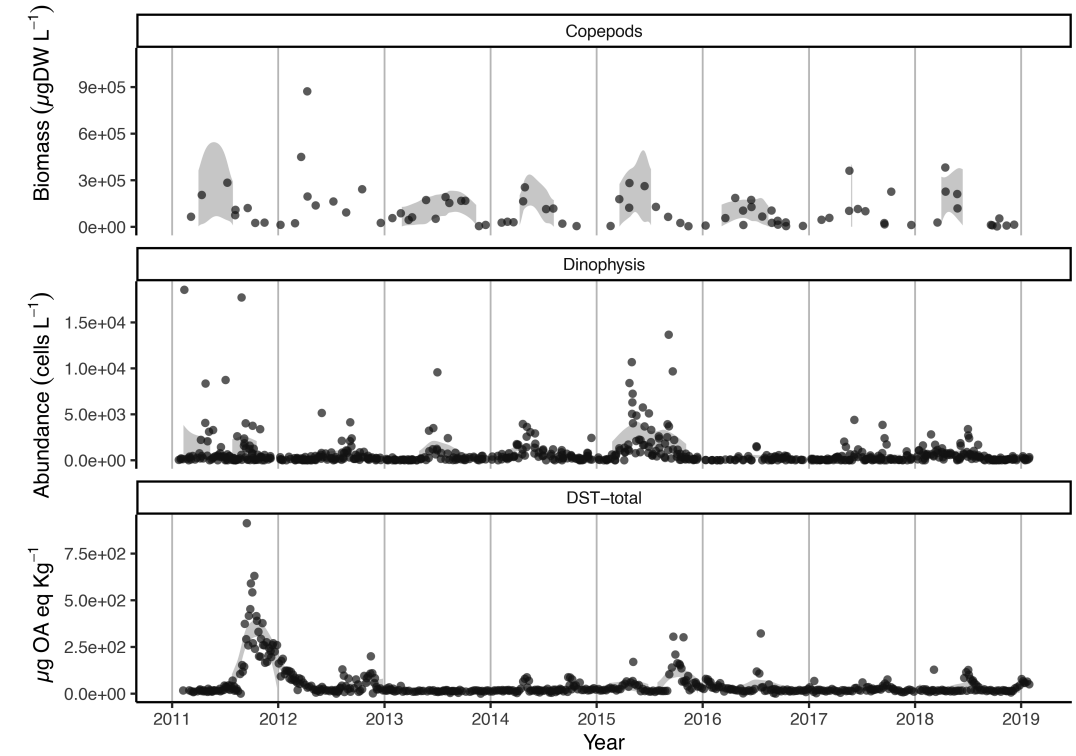

Fig. 3. Seasonal variation of DST-total concentration in mussels, copepod biomass, and *Dinophysis* spp. abundance over 8 yr from the Swedish West Coast.

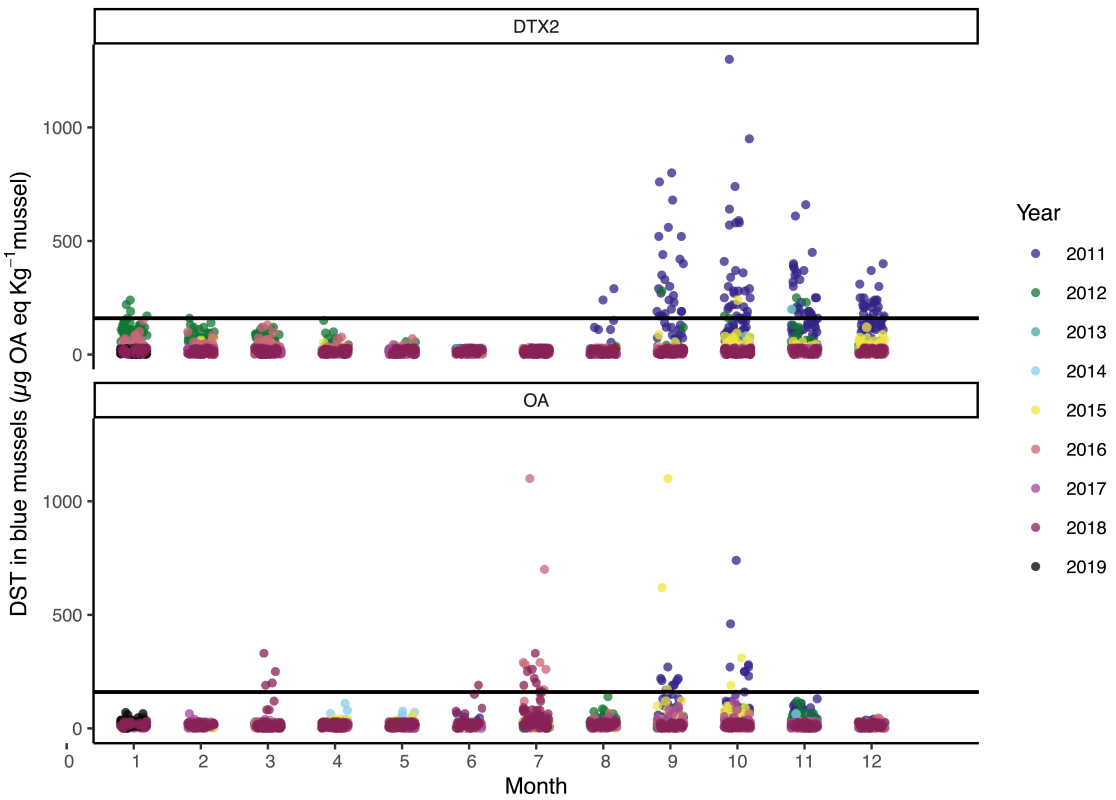

Fig. 4. Concentration OA, and DTX-2 in blue mussels from the Swedish West Coast between January 2011 and January 2019. Years are denoted by color, and EU regulatory level of 160 μg OA eq kg^{-1} mussel is indicated with a horizontal line.

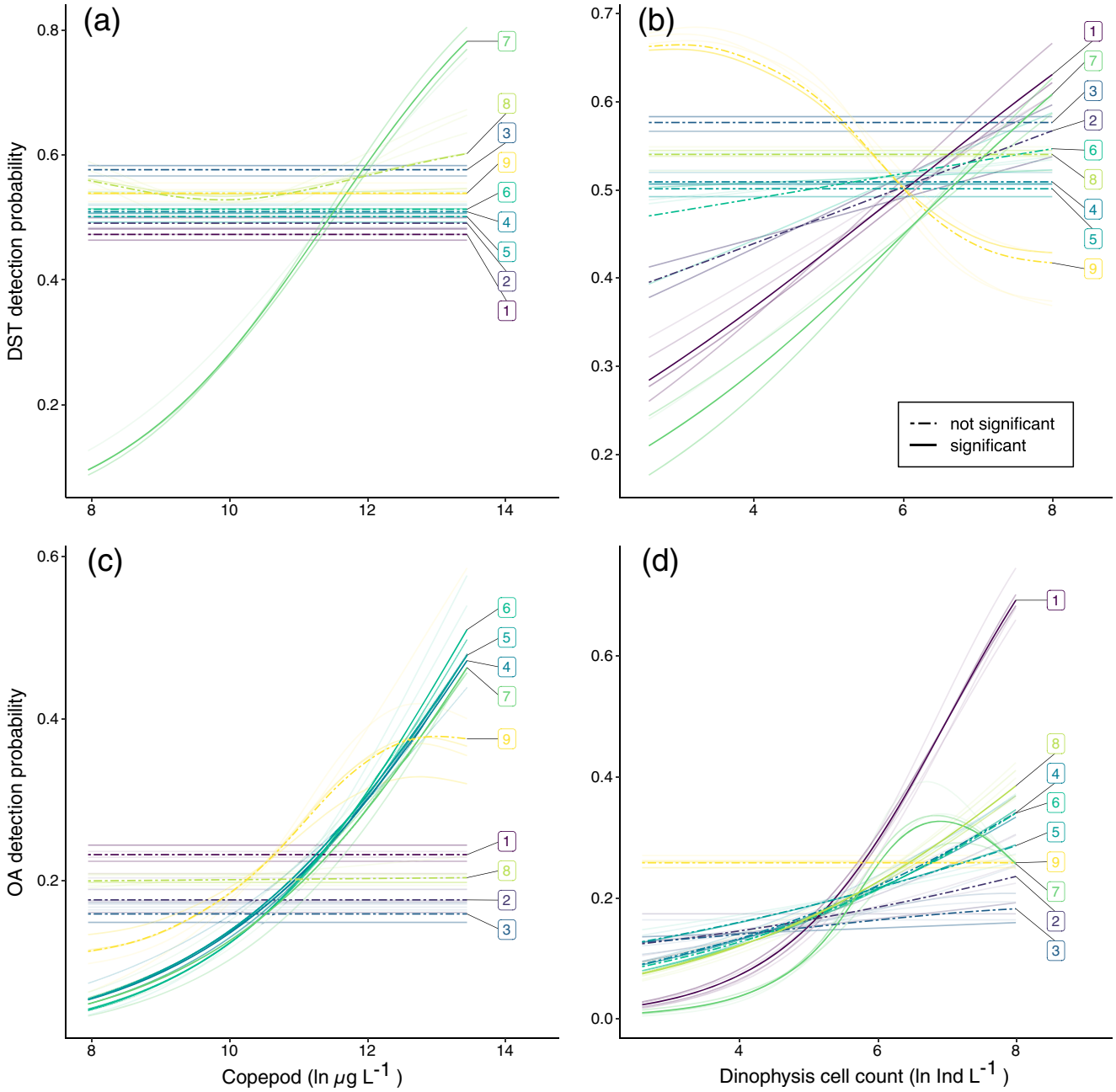

Fig. 5. Top: DST-total detection probability as a function of (**a**) copepod and (**b**) *Dinophysis* cell counts. Bottom: OA detection probability as a function of (**c**) copepod biomass in mussels and (**d**) *Dinophysis* cell counts. Different community response times spanning 1–9 weeks are indicated by color. Bold lines represent the averaged model predictions, and faint lines show individual model predictions from a binomial generalized additive model.

the model for OA and DST-total (Fig. 5). Models including copepod data also generally improved the amount of explained variance, compared to a model that only included *Dinophysis* abundance as the explanatory variable (Table 1).

Contrary to the binomial models, we could not detect any significant relationships in models which used the toxin concentration (DST-total or OA) as a dependent factor with copepod biomass and *Dinophysis* cell counts as explanatory factors, but models with *Dinophysis* alone revealed a significant relationship. DTX-2 was not influenced by any of the explanatory factors in the binomial model looking at the presence and absence of the toxin or the model predicting the toxin concentration. Model coefficients for both binomial and lognormal models, toxins, and all community response durations can be found in the Supporting Information Appendix S4.

Table 1. Averaged model coefficients and adjusted R^2 from generalized additive models predicting (a) the detection probability and (b) the concentration of DST-total, OA, and DTX-2 for a 4-week community response time, a model without copepod biomass, and for the response time which explained most of the variance in the data. s(Cop) is the smooth term for copepod biomass and s(Dino) represents the smooth term for *Dinophysis*. Averages are from 10 runs. Coefficients for models with other response times can be found in the Supporting Information Appendix S4. Estimated degrees of freedom (edf) indicate the complexity of the smooth function. Bold terms indicate significant model predictions ($p < 0.05$).

a. Modeling the detection of microalgal toxins (presence/absence)

Model	Cop lag	Dino lag	Parameter	edf	Chi.sq	*p* value	R^2
DST-total ~ s(Cop) + s(Dino)	4	1	s(Cop)	0	0	0.499	0
	4	1	s(Dino)	0	0	0.659	
DST-total ~ s(Cop) + s(Dino)	**7**	**1**	**s(Cop)**	**0.87**	**5.86**	**0.01**	**0.16**
	7	**1**	**s(Dino)**	**0.81**	**3.41**	**0.042**	
DST-total ~ s(Dino)		1	s(Dino)	0.57	1.43	0.127	0
OA ~ s(Cop) + s(Dino)	**4**	**1**	**s(Cop)**	**0.78**	**3.16**	**0.043**	**0.1**
	4	1	s(Dino)	0.73	2.42	0.065	
OA ~ s(Cop) + s(Dino)	**7**	**1**	**s(Cop)**	**0.78**	**3.07**	**0.048**	**0.2**
	7	**1**	**s(Dino)**	**1.8**	**5.58**	**0.034**	
OA ~ s(Dino)		**1**	**s(Dino)**	**0.94**	**15.24**	**<0.001**	**0.06**
DTX2 ~ s(Cop) + s(Dino)	4	1	s(Cop)	0.21	0.26	0.263	0
	4	1	s(Dino)	0	0	0.501	
DTX2 ~ s(Cop) + s(Dino)	2	1	s(Cop)	1.29	2.68	0.133	0.09
	2	1	s(Dino)	1.59	3.7	0.094	
DTX2 ~ s(Dino)		1	s(Dino)	1.05	3.11	0.056	0.01

b. Modeling the concentration of microalgal toxins

Model	Cop lag	Dino lag	Parameter	edf	*F*	*p* value	R^2
DST-total ~ s(Cop) + s(Dino)	4	1	s(Cop)	0.09	0.03	0.6035	0.02
	4	1	s(Dino)	0.42	0.1	0.2455	
DST-total ~ s(Cop) + s(Dino)	7	1	s(Cop)	0.66	0.31	0.1195	0.08
	7	1	s(Dino)	0.71	0.26	0.1128	
DST-total ~ s(Dino)		1	s(Dino)	0.85	0.54	0.052	0.02
OA ~ s(Cop) + s(Dino)	4	1	s(Cop)	0.61	0.31	0.1657	0.09
	4	1	s(Dino)	0.7	0.35	0.3161	
OA ~ s(Cop) + s(Dino)	7	1	s(Cop)	0.71	0.46	0.1973	0.1
	7	1	s(Dino)	0.83	0.29	0.1667	
OA ~ s(Dino)		**1**	**s(Dino)**	**0.96**	**1.1**	**0.005**	**0.03**
DTX2 ~ s(Cop) + s(Dino)	4	1	s(Cop)	0.17	0.04	0.5982	0.01
	4	1	s(Dino)	0.23	0.06	0.3781	
DTX2 ~ s(Cop) + s(Dino)	1	1	s(Cop)	0.07	0.01	0.5635	0.05
	1	1	s(Dino)	1	0.45	0.2379	
DTX2 ~ s(Dino)		1	s(Dino)	0.08	0.02	0.69	0

Modeling biotoxins using copepodamides in mussels

Copepodamide concentration in mussels from the Swedish West Coast fluctuated between May and December, 2018. Samples contained a mixture of active intact and degraded lyso-copepodamide structures (Fig. 6a). Lyso-copepodamides, which do not elicit defensive responses, made up more than 70% of the total copepodamide concentration in each sample over the whole study period. Week 18 (29 April–05 May) had the greatest proportion of intact copepodamides, but they were still only 25–30% of the total copepodamide concentration. By week 30 (22–28 July), intact structures had declined to less than 0.5% of the copepodamide content in mussels and remained at low levels until week 40 (01–07 October). Intact copepodamides increased again after week 40, reaching approximately 15% of the total concentration by the end of the year. The increase may have been aided by cooler water temperatures, which slows the degradation from active copepodamides to inactive lyso-structures (Selander

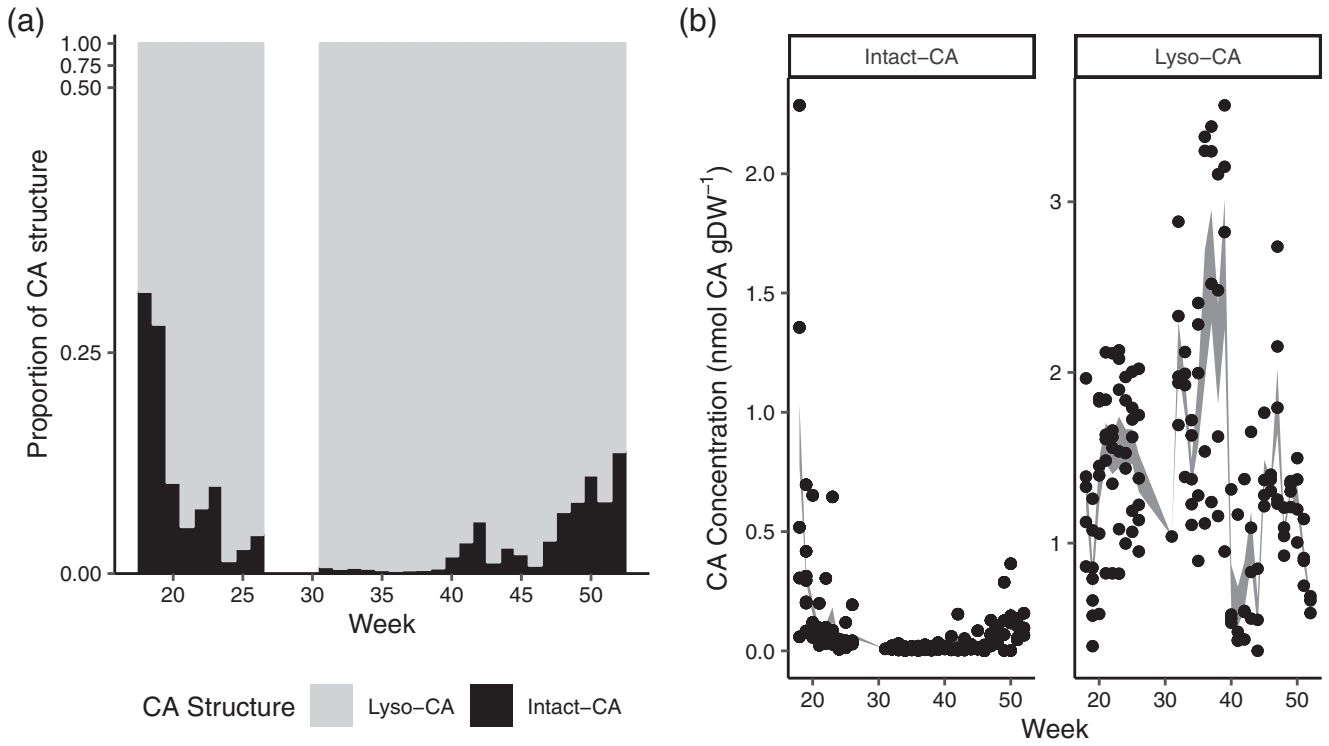

Fig. 6. (**a**) Proportion of intact copepodamide (Intact-CA) to lyso-copepodamides (Lyso-CA) structures in extracts from blue mussels. Data shows weekly mean across all sampling locations. (**b**) Seasonal variation of copepodamide concentration in blue mussels. Shaded region gives mean ± SE. Mussel samples were unavailable for weeks 27–31.

Table 2. Averaged model coefficients and adjusted R^2 from generalized additive models predicting either DST-total or OA for a 4-week community response time, a model without copepodamides, and for the lead time which explained most of the variance in the data. s(CA) is the smooth term for copepodamides and s(Dino) represents the smooth term for Dinophysis. Each model was run 10 times. Results for all other responses can be found in the Supporting Information Appendix S5. edf represents the estimated degrees of freedom of the model terms, which indicates the complexity of the smooth function. Bold terms indicate significant model predictions ($p < 0.05$).

Model	CA lag	Dino lag	Parameter	edf	*F*	*p* value	R^2
DST-total ~ s(CA) + s(Dino)	**4**	**1**	**s(CA)**	**2.19**	**1.47**	**0.0062**	**0.58**
	4	**1**	**s(Dino)**	**1.58**	**0.73**	**0.0358**	
DST-total ~ s(CA) + s(Dino)	**7**	**1**	**s(CA)**	**1.1**	**6.05**	**<0.0001**	**0.76**
	7	1	s(Dino)	0.53	0.12	0.2762	
DST-total ~ s(Dino)		1	s(Dino)	0.62	0.22	0.1107	0.05
OA ~ s(CA) + s(Dino)	4	1	s(CA)	0.94	0.34	0.2664	0.45
	4	**1**	**s(Dino)**	**1.92**	**1.32**	**0.0079**	
OA ~ s(CA) + s(Dino)	**9**	**1**	**s(CA)**	**2.35**	**5.27**	**0.0002**	**0.73**
	9	1	s(Dino)	0.42	0.14	0.3812	
OA ~ s(Dino)		**1**	**s(Dino)**	**1.21**	**0.58**	**0.0344**	**0.13**

et al. 2019). The mean weekly concentration of intact copepodamides followed the same pattern (Fig. 6b).

For the estimated 4-week community response time to copepodamides, we detected a significant relationship between copepodamide and DST-total, but not OA (Table 2). Using a longer lead time (DST 7 weeks and OA 9 weeks) increased the explanatory value and diminished the role of *Dinophysis* spp. cell counts in both models (Fig. 7).

Copepodamide accumulation and depuration experiments

To confirm that copepod cues extracted from mussels were accumulated from the water, live blue mussels were exposed to a

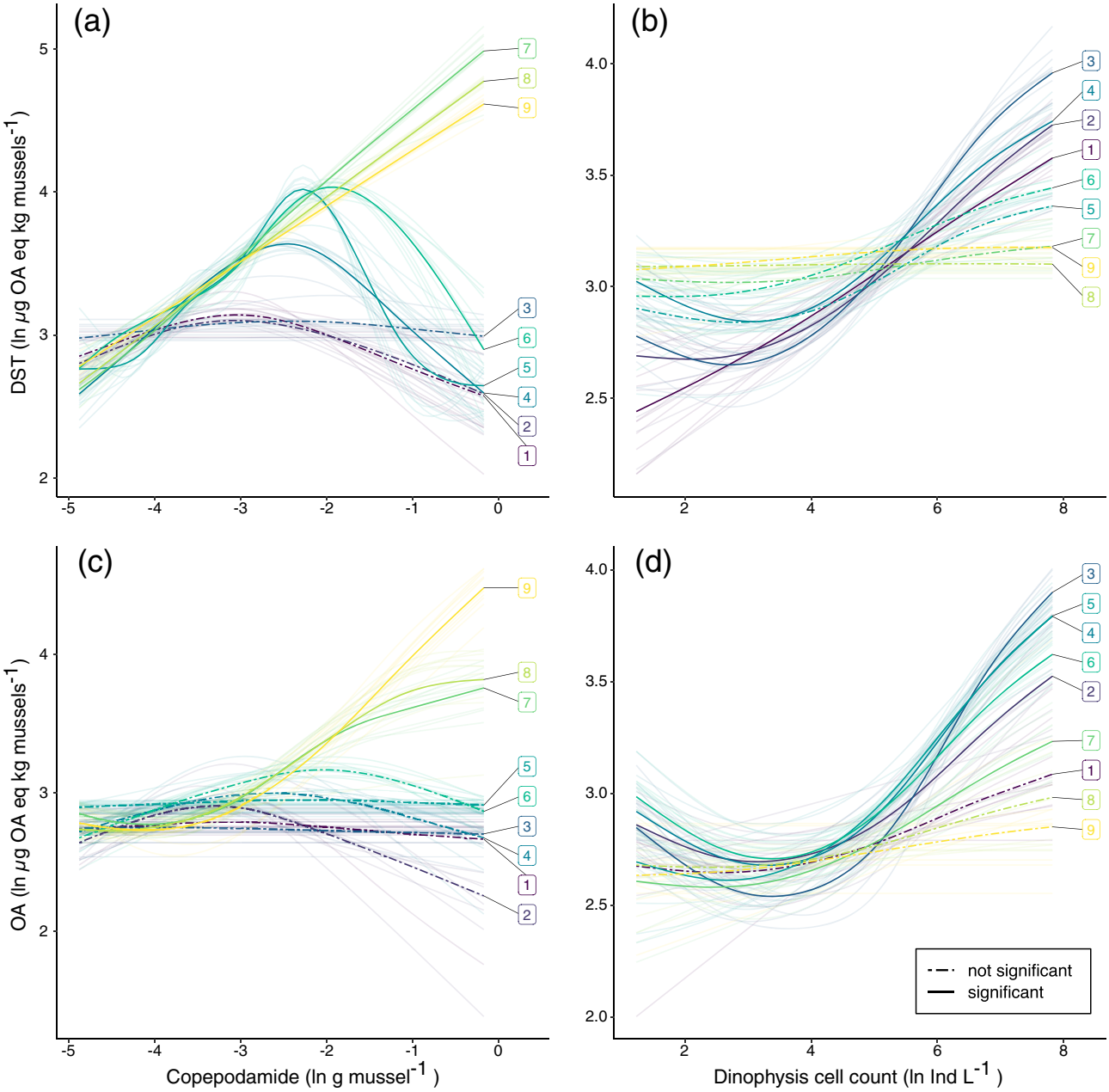

Fig. 7. Top: DST-total concentration in blue mussels as a function of (**a**) copepodamide and (**b**) *Dinophysis* spp. cell counts. Bottom: OA concentration in blue mussels as a function of (**c**) copepodamide and (**d**) *Dinophysis* cell counts. Potential lead times from 1 to 9 weeks are indicated by color. Bold lines represent the averaged model predictions and faint lines show individual model predictions.

1 nmol L^{-1} concentration of copepodamides. The mean copepodamide content in mussels increased by 10.7 ± 0.1 pmol gDW^{-1} after 12 h (Fig. 8a, $p << 0.01$). Copepodamides deacylate naturally in seawater, degrading from chemically active intact structures to inactive lyso-copepodamide structures over time. Deacylation likely contributed to the minute increase of lyso structures in copepodamide (CA +) treatment relative to copepodamide negative (CA −) treatment after 12 h (Fig. 8b).

About 1.6 pmol L^{-1} residual copepodamides were detected in the water after 12 h, or 0.16% of the initial amount (Fig. 8b). Since the added copepodamide mix included only intact copepodamides, it is likely that the lyso-copepodamides remaining in the water were degradation products. About 10.5% of the added copepodamide was recovered from the mussel extracts.

Copepodamide depuration experiments

To estimate the timescale of copepodamide depuration in mussels, *M. edulis* kept in copepodamide-free seawater, were sampled over a 96 h period. The total mean copepodamide concentration

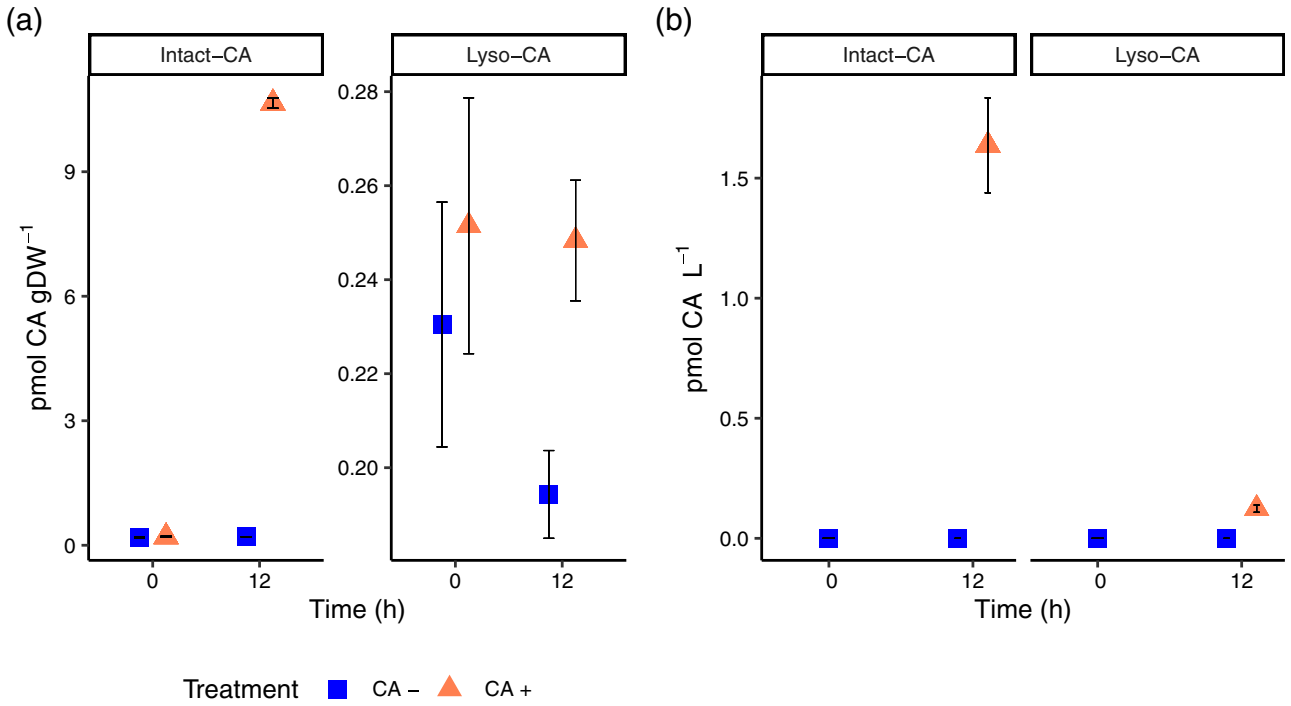

Fig. 8. (**a**) Accumulation of intact copepodamides (Intact-CA) and lyso-copepodamides (Lyso-CA) over 12 h from blue mussels dosed with 1 nmol L^{-1} copepodamides (CA+) and methanol (CA−). (**b**) Copepodamide concentration remaining in the water after 12 h. All data show mean ± SE (pmol CA gDW^{-1}) mussel ($n = 3$).

decreased from 2.1 ± 0.5 to 0.01 ± 0.05 nmol CA gDW^{-1} (± standard error [SE], $p << 0.01$) for intact copepodamides and 40 ± 7 to 13 ± 2 nmol CA gDW^{-1} (± SE) for lyso-copepodamides. Linear regression of the concentration at each time point gave a half-life of 35 h for intact copepodamides and 81 h for lyso-copepodamides (Fig. 9).

Discussion

We aimed to test if accuracy and lead time for predicting algal toxins in aquaculture can be improved by including information about copepod biomass or copepodamides extracted from mussels. This is in line with recent recommendations for a global HAB observing system that couples bloom dynamics with ocean observations to develop new prediction strategies (Anderson et al. 2019). Eavesdropping on zooplankton, as dominating dinoflagellate predators, may foreshadow increasing levels of microalgal toxins and upcoming changes in phytoplankton community composition.

Results suggest that copepod biomass and copepodamide concentration are correlated to future DST events in mussels, especially OA, with 1–2 months of lead time. Interestingly, our initial estimation of a 4-week time lag, illustrated in Fig. 1 as the community response of harmful taxa to copepod grazers, seems too short. Extending the period between grazer presence and toxins improved the explanatory power of most models. It is possible that the advantage conferred to harmful taxa from selective grazing by copepods is only marginally larger than the difference in growth rate between defended dinoflagellates and nondefended competitors. However, our results should be interpreted with caution as they are based on correlative evidence alone and were limited by the availability and scope of consistent plankton monitoring.

There is convincing evidence that *Dinophysis* cells are better correlated to DST concentration in shellfish when standardized to co-occurring nontoxic cells because shellfish accumulate more toxins when harmful algae are a greater proportion of the total food available (Sampayo et al. 1990; Moroño et al. 2001; Reguera et al. 2014). A review by Blanco (2018) describes the quantitative relationships that affect the uptake rate of DST. Uptake kinetics models include variables for feeding rate and absorption efficiency, which can vary depending on the total volume of consumed particles (Blanco 2018). Future work in shellfish production areas that also measure chlorophyll could standardize to the total phytoplankton abundance by applying weighted (chlorophyll a)$^{-2}$ as described in Dahl and Johannessen (2001) to the model instead of simple cell counts.

Other factors known to affect *Dinophysis* growth rates and toxin profiles will likely contribute to the timescale of a community response to grazers. Conditions that enhance the relative proportion of toxic cells and per cell toxin content may shorten the response time between grazer cues and the accumulation of biotoxins in mussels. For example, as a

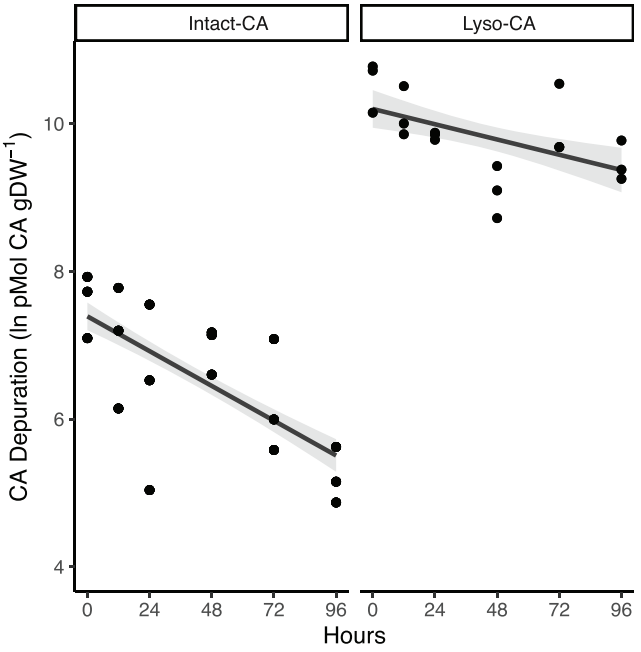

Structure	Slope	$T_{1/2}$ (h)	R^2	*p value*
Lyso-CA	-0.009	80.5	0.24	0.021
Intact-CA	-0.02	35.3	0.44	0.001

Fig. 9. Depuration over 96 h for intact copepodamides (Intact-CA) and lyso-copepodamides (Lyso-CA). Data are shown with linear regression and shaded SE. Table summary of regression statistics and half-life ($T_{1/2}$).

mixotrophic genera, *Dinophysis* spp. growth and intracellular toxin content are linked to the availability and nutrient content of ciliate prey (Nielsen et al. 2013; Smith et al. 2018). When prey is not limiting, nitrogen loading from ammonium and organic matter promotes growth of *D. acuminata* in coastal ecosystems (Seeyave et al. 2009; Hattenrath-Lehmann and Gobler 2015). Eutrophication would be likely to shift the model in the event of an increase in the ratio of *Dinophysis* to the total volume of seston consumed by bivalve mollusks (Blanco 2018). Another complexity comes from *Dinophysis* field studies that show an inverse relationship between cell density and toxins (Lindahl et al. 2007), and later experiments in culture show that per cell toxin content varies strongly with growth phase (Tong et al. 2011). Rigorous laboratory and field studies are needed to further elucidate the relative impact and timescale of ecological interactions, such as selective grazing, allelopathy, nutrients, and prey availability, on *Dinophysis* bloom dynamics.

The relationship between copepodamides and toxin content in mussels is stronger than the relationship between copepods and toxin content. This suggests that copepodamide measurements may be the better predictor. In the long-term data set, we used an overall average copepod biomass for the whole region, whereas the copepodamides reflect the integrated past copepod biomass in the water where the mussels were feeding. Moreover, copepod measurements were recorded monthly on SHARKweb, and only two stations were centered in the study region. Phytoplankton and toxins were reported weekly from at least 20 different stations. This sampling imbalance introduced spatial and temporal gaps in our long-term analysis, but it should not affect our short-term analysis using copepodamides. By sampling copepods more frequently and in closer proximity to the shellfish farms, it is likely that the models could be improved, but zooplankton sampling is costly and time-consuming. This limitation makes copepodamide analysis in mussel extracts an appealing alternative. Ultimately, validation of a method including grazers cannot rely on public monitoring systems alone and requires more control over sampling location and time-interval.

In addition to the predictive and logistical advantages over copepod monitoring, extracting copepodamides from mussels also has advantages over direct copepodamide measurements from seawater. Solid phase extraction of dissolved copepodamides is sensitive to time and temperature. In a study by Selander et al. (2019), the effective concentration of intact copepodamides in seawater decreased by half in less than 3 h at 15°C with near complete degradation after 24 h. The half-life of copepodamides in mussels was determined to be about 35 h. Moreover, copepodamides are analyzed with the same LCMS/MS methods commonly used in biotoxin monitoring to replace or supplement traditional bioassays. Monitoring programs that already require analysis of lipophilic extracts by LCMS/MS, e.g. EU 15/2011, could analyze copepodamides from mussels with minimal extra effort (European Commission, 2011).

A modification to solid phase adsorption toxin tracking (SPATT; MacKenzie et al. 2004) could be another potential, cost-effective method for in situ copepodamide monitoring. SPATT, which deploys synthetic resins to adsorb free toxins from the water column, has been used successfully in freshwater and marine environments for diverse toxin structures (Kudela 2011; Li et al. 2016; Roué et al. 2018). Lipophilic toxins are especially efficacious with SPATT, and multiple resins have been developed to adsorb DSTs (MacKenzie et al. 2004; Fux et al. 2009). Benefits of toxin tracking with SPATT include low cost, ease of storage and transport, use in areas without naturally occurring shellfish, and no matrix effects or biotransformation from shellfish (MacKenzie 2010). However, tests using SPATT as an early warning for DSTs found that passive samplers and shellfish accumulated toxins at nearly the same time (Fux et al. 2009; Pizarro et al. 2013), and a study by Li et al. (2016) could not conclude that SPATT was an efficient tool for early warning of DST in Lingshan Bay scallops. Copepodamides, as lipophilic exudates, may be an

ideal fit for passive sampling. In addition to the other benefits of SPATT over shellfish extracts, the results of this study suggest that adapting SPATT technology for grazer cues has the potential to improve both precision and lead time compared to tracking biotoxins alone.

Dinoflagellates have low maximum growth rates and are poor competitors for nutrients compared to similar sized taxa (Banse 1982). As a consequence, they probably depend on other advantages, such as allelochemicals (Fistarol et al. 2004) and selective grazers to suppress their competitors (Irigoien et al. 2005; Prevett et al. 2019). Under the right conditions, this relationship can increase local toxin accumulation in shellfish by enriching harmful taxa through selective grazing and grazer induced toxin formation. Selective rejection of harmful taxa is well supported in some species and less supported in others, leaving many predator–prey interactions still poorly understood (Turner 2014; Xu and Kiørboe 2018). There are also conflicting reports on the effects of algae toxins on copepods. Both negative and neutral effects of paralytic shellfish toxins (PSTs) on copepods have been observed. For example, Turner and Borkman (2005) found no adverse effects of toxic *Alexandrium* sp. on grazers after 24 h, whereas other studies with *Alexandrium* found depressed feeding, hatching, and larval development of copepods and even direct mortality (Teegarden 1999; Frangopulos et al. 2000; Colin and Dam 2003).

Understanding of predator-prey interactions between copepods and *Dinophysis* spp. is less developed than for PST producing dinoflagellates such as *Alexandrium* spp. However, there is some evidence that OA produced by *D. acuta* repels copepod grazers (Carlsson et al. 1995), and *Temora* sp. copepods reject *D. acuminata* 60% more often than a nontoxic controls (Xu and Kiørboe 2018). In opposition, Wexels Riser et al. (2003) found that *Calanus* spp. copepods fed readily on OA producing *D. norvegica*, accumulating toxins with seemingly no adverse effects, and a study on plankton assemblages from the Baltic Sea concluded that grazing copepods could have a negative impact on *Dinophysis* spp. blooms during poor growth conditions (Kozlowsky-Suzuki et al. 2006). In addition, copepod populations that are historically exposed to HABs may show less selective feeding behavior than copepods that do not naturally co-occur with toxic algae, and preferences could be population- or strain-specific (Colin and Dam 2002). This kind of ecological "arms race," whereby prey become more toxic and grazers become more resistant could also be at play in the Swedish West Coast system. Culture experiments would likely be necessary to observe an alternative selection mechanism that favors OA-group resistant copepods due to the characteristically low density of natural *Dinophysis* blooms.

In the North Atlantic, copepod production usually peaks twice per year; after the spring phytoplankton bloom near April and at the end of November (Lindahl and Hernroth 1983; O'Brien et al. 2013). This pattern is consistent with the seasonal variation of extracted copepodamides, but copepod monitoring data were too scarce to make a direct comparison between copepod biomass and copepodamide concentration in mussels. Mussels were observed taking up copepodamides from the water in the accumulation experiment. Under controlled conditions, simple mathematical models like those used to explain kinetics of DSP toxins in *Mytilus galloprovincialis* (Moroño et al. 2003) may help to link copepod density to copepodamides accumulated in mussels. The copepodamide contribution that could accumulate from predation by mussels on smaller copepod species is still unknown (Lehane and Davenport 2006; Jonsson et al. 2009).

The three predominant toxic species of *Dinophysis* in the study region are *D. acuta*, *D. acuminata*, and *D. norvegica* (Karlson et al. 2007; Johansen and Rundberget 2008). All species produce OA and DTX-1, and only *D. acuta* has been observed producing DTX-2 (Johansen and Rundberget 2008). No DTX-1 was detected during the study period, and *D. acuta* was the least abundant *Dinophysis* contributor (S1). This may explain why the model was most successful at predicting OA and DST-total in mussels and found no significant results for DTX-2. Field populations of *D. acuta* produce OA and DTX-2 at a ratio of approximately 3:2 (Pizarro et al. 2009), so a species-specific analysis including grazers with *D. acuta* might be more promising for predicting DTX-2. However, the leading OA-group toxin threat on the Swedish West Coast appears to shift from DTX-2 to OA after 2014 (Fig. 4), so a predictive model that focuses on a combined DST-total measurement might be the most attractive for monitoring efforts in this region.

Next generation HAB forecasting is expanding to include additional biotic and abiotic factors, establishing a more complete picture of toxin drivers. For the first time, we show the history of copepod density correlates to elevated toxin content in farmed mussels. While selective grazing and grazer induced toxin formation may explain this pattern in other harmful dinoflagellates, they have yet to be tested for DST and *Dinophysis*. Preliminary results suggest measuring the accumulation of copepodamides, a group of copepod derived toxin elicitors, is a novel and cost-efficient way to include past grazing intensity in new efforts to understand and forecast harmful algal blooms.

References

Anderson, C. R., R. M. Kudela, M. Kahru, Y. Chao, L. K. Rosenfeld, F. L. Bahr, D. M. Anderson, and T. A. Norris. 2016. Initial skill assessment of the California Harmful Algae Risk Mapping (C-HARM) system. Harmful Algae **59**: 1–18. doi:10.1016/j.hal.2016.08.006

Anderson, C. R., and others. 2019. Scaling up from regional case studies to a global harmful algal bloom observing system. Front. Mar. Sci. **6**: 250. doi:10.3389/fmars.2019.00250

Banse, K. 1982. Cell volumes, maximal growth rates of unicellular algae and ciliates, and the role of ciliates in the marine pelagial 1,2. Limnology and Oceanography **27**: 1059–1071. http://dx.doi.org/10.4319/lo.1982.27.6.1059

Bjærke, O., P. R. Jonsson, A. Alam, and E. Selander. 2015. Is chain length in phytoplankton regulated to evade predation? J. Plankton Res. **37**: 1110–1119. doi:10.1093/plankt/fbv076

Blanco, J. 2018. Accumulation of Dinophysis toxins in bivalve molluscs. Toxins **10**: 453. doi:10.3390/toxins10110453

Carlsson, P., E. Granéli, G. Finenko, and S. Y. Maestrini. 1995. Copepod grazing on a phytoplankton community containing the toxic dinoflagellate *Dinophysis acuminata*. J. Plankton Res. **17**: 1925–1938. doi:10.1093/plankt/17.10.1925

Colin, S. P., and H. G. Dam. 2002. Latitudinal differentiation in the effects of the toxic dinoflagellate *Alexandrium* spp. on the feeding and reproduction of populations of the copepod *Acartia hudsonica*. Harmful Algae **1**: 113–125. doi:10.1016/S1568-9883(02)00007-0

Colin, S. P., and H. G. Dam. 2003. Effects of the toxic dinoflagellate *Alexandrium fundyense* on the copepod *Acartia hudsonica*: A test of the mechanisms that reduce ingestion rates. Mar. Ecol. Prog. Ser. **248**: 55–65. doi:10.3354/meps248055

Dahl, E., and T. Johannessen. 2001. Relationship between occurrence of Dinophysis species (Dinophyceae) and shellfish toxicity. Phycologia **40**: 223–227. doi:10.2216/i0031-8884-40-3-223.1

Davidson, K., D. M. Anderson, M. Mateus, B. Reguera, J. Silke, M. Sourisseau, and J. Maguire. 2016. Forecasting the risk of harmful algal blooms. Harmful Algae **53**: 1–7. doi:10.1016/j.hal.2015.11.005

European Commission. 2011. Commission Regulation (EU) No 15/2011 of 10 January 2011 amending Regulation (EC) No 2074/2005 as regards recognised testing methods for detecting marine biotoxins in live bivalve molluscs. Off. J. Eur. Union **6**: 3–6. doi:10.3000/17252555.L_2011.006.eng

Fistarol, G. O., C. Legrand, E. Selander, C. Hummert, W. Stolte, and E. Granéli. 2004. Allelopathy in *Alexandrium* spp.: Effect on a natural plankton community and on algal monocultures. Aquat. Microb. Ecol. **35**: 45–56. doi:10.3354/ame035045

Frangopulos, M., C. Guisande, I. Maneiro, I. Riveiro, and J. Franco. 2000. Short-term and long-term effects of the toxic dinoflagellate *Alexandrium minutum* on the copepod *Acartia clausi*. Mar. Ecol. Prog. Ser. **203**: 161–169. doi:10.3354/meps203161

Fux, E., R. Bire, and P. Hess. 2009. Comparative accumulation and composition of lipophilic marine biotoxins in passive samplers and in mussels (*M. edulis*) on the West Coast of Ireland. Harmful Algae **8**: 523–537. doi:10.1016/j.hal.2008.10.007

Godhe, A., S. Svensson, and A. S. Rehnstam-Holm. 2002. Oceanographic settings explain fluctuations in *Dinophysis* spp. and concentrations of diarrhetic shellfish toxin in the plankton community within a mussel farm area on the Swedish west coast. Mar. Ecol. Prog. Ser. **240**: 71–83. doi:10.3354/meps240071

Grasso, I., S. D. Archer, C. Burnell, B. Tupper, C. Rauschenberg, K. Kanwit, and N. R. Record. 2019. The hunt for red tides: Deep learning algorithm forecasts shellfish toxicity at site scales in coastal Maine. Ecosphere **10**: 1–11. doi:10.1002/ecs2.2960

Grebner, W., E. C. Berglund, F. Berggren, J. Eklund, S. Harðadóttir, M. X. Andersson, and E. Selander. 2019. Induction of defensive traits in marine plankton—new copepodamide structures. Limnol. Oceanogr. **64**: 820–831. doi:10.1002/lno.11077

Hattenrath-Lehmann, T., and C. J. Gobler. 2015. The contribution of inorganic and organic nutrients to the growth of a North American isolate of the mixotrophic dinoflagellate, *Dinophysis acuminata*. Limnol. Oceanogr. **60**: 1588–1603. doi:10.1002/lno.10119

Hill, P. R., A. Kumar, M. Temimi, and D. R. Bull. 2020. HABNet: Machine learning, remote sensing-based detection of harmful algal blooms. IEEE J. Sel. Top. Appl. Earth Obs. Remote Sens. **13**: 3229–3239. doi:10.1109/JSTARS.2020.3001445

Hong, Y., M. A. Burford, P. J. Ralph, J. W. Udy, and M. A. Doblin. 2013. The cyanobacterium *Cylindrospermopsis raciborskii* is facilitated by copepod selective grazing. Harmful Algae **29**: 14–21. doi:10.1016/j.hal.2013.07.003

Humbert, J. F., C. Quiblier, and M. Gugger. 2010. Molecular approaches for monitoring potentially toxic marine and freshwater phytoplankton species. Anal. Bioanal. Chem. **397**: 1723–1732. doi:10.1007/s00216-010-3642-7

Irigoien, X., K. J. Flynn, and R. P. Harris. 2005. Phytoplankton blooms: A 'loophole' in microzooplankton grazing impact? J. Plankton Res. **27**: 313–321. doi:10.1093/plankt/fbi011

Jang, M. H., K. Ha, G. J. Joo, and N. Takamura. 2003. Toxin production of cyanobacteria is increased by exposure to zooplankton. Freshw. Biol. **48**: 1540–1550. doi:10.1046/j.1365-2427.2003.01107.x

Johansen, M., and T. Rundberget. 2008. Differences in toxin composition and toxin content within and between species of the genus Dinophysis, with special emphasis on *D. acuta*. Gothenburg Univ.

Jonsson, A., T. G. Nielsen, I. Hrubenja, M. Maar, and J. K. Petersen. 2009. Eating your competitor: Functional triangle between turbulence, copepod escape behavior and predation from mussels. Mar. Ecol. Prog. Ser. **376**: 143–151. doi:10.3354/meps07817

Karlson, B., A.-S. Rehnstam-Holm, and L. Loo. 2007. Temporal and spatial distribution of diarrhetic shellfish toxins in blue mussels, *Mytilus edulis* (L.), on the Swedish west coast, NE Atlantic, 1988–2005. Swedish Meteorological and Hydrological Institute, Reports Oceanography, no 35, 40 pp.

Kozlowsky-Suzuki, B., P. Carlsson, A. Rühl, and E. Granéli. 2006. Food selectivity and grazing impact on toxic *Dinophysis* spp. by copepods feeding on natural plankton

assemblages. Harmful Algae **5**: 57–68. doi:10.1016/j.hal.2005.05.002

Kudela, R. M. 2011. Characterization and deployment of Solid Phase Adsorption Toxin Tracking (SPATT) resin for monitoring of microcystins in fresh and saltwater. Harmful Algae **11**: 117–125. doi:10.1016/j.hal.2011.08.006

Lehane, C., and J. Davenport. 2006. A 15-month study of zooplankton ingestion by farmed mussels (*Mytilus edulis*) in Bantry Bay, Southwest Ireland. Estuar. Coast. Shelf Sci. **67**: 645–652. doi:10.1016/j.ecss.2005.12.015

Li, F. L., Z. X. Li, M. M. Guo, H. Y. Wu, T. T. Zhang, and C. H. Song. 2016. Investigation of diarrhetic shellfish toxins in Lingshan Bay, Yellow Sea, China, using solid-phase adsorption toxin tracking (SPATT). Food Addit. Contam. Part A Chem. Anal. Control Expo. Risk Assess. **33**: 1367–1373. doi:10.1080/19440049.2016.1200752

Lindahl, O., Lundve, B., and Johansen, M. 2007. Toxicity of Dinophysis spp. in relation to population density and environmental conditions on the Swedish west coast. Harmful Algae **6**: 218–231. http://dx.doi.org/10.1016/j.hal.2006.08.007

Lindahl, O., and L. Hernroth. 1983. Phyto-zooplankton community in coastal waters of western Sweden—an ecosystem off balance? Mar. Ecol. Prog. Ser. **10**: 119–126. doi:10.3354/meps010119

Lindegarth, S., T. Torgersen, B. Lundve, and M. Sandvik. 2009. Differential retention of okadaic acid (OA) group toxins and pectenotoxins (PTX) in the blue mussel, *Mytilus edulis* (L.), and European flat oyster, *Ostrea edulis* (L.). J. Shellfish Res. **28**: 313–323. doi:10.2983/035.028.0213

Lindström, J., W. Grebner, K. Rigby, and E. Selander. 2017. Effects of predator lipids on dinoflagellate defence mechanisms - increased bioluminescence capacity. Sci. Rep. **7**: 13104. doi:10.1038/s41598-017-13293-4

MacKenzie, L., V. Beuzenberg, P. Holland, P. McNabb, and A. Selwood. 2004. Solid phase adsorption toxin tracking (SPATT): A new monitoring tool that simulates the biotoxin contamination of filter feeding bivalves. Toxicon **44**: 901–918. doi:10.1016/j.toxicon.2004.08.020

MacKenzie, L. A. 2010. In situ passive solid-phase adsorption of micro-algal biotoxins as a monitoring tool. Curr. Opin. Biotechnol. **21**: 326–331. doi:10.1016/j.copbio.2010.01.013

Moroño, A., J. Franco, M. Miranda, M. I. Reyero, and J. Blanco. 2001. The effect of mussel size, temperature, seston volume, food quality and volume-specific toxin concentration on the uptake rate of PSP toxins by mussels (*Mytilus galloprovincialis* Lmk). J. Exp. Mar. Biol. Ecol. **257**: 117–132. doi:10.1016/S0022-0981(00)00336-1

Moroño, A., F. Arévalo, M. L. Fernández, J. Maneiro, Y. Pazos, C. Salgado, and J. Blanco. 2003. Accumulation and transformation of DSP toxins in mussels *Mytilus galloprovincialis* during a toxic episode caused by *Dinophysis acuminata*. Aquat. Toxicol. **62**: 269–280. doi:10.1016/S0166-445X(02)00105-4

Naustvoll, L. J., E. Gustad, and E. Dahl. 2012. Monitoring of Dinophysis species and diarrhetic shellfish toxins in Flødevigen Bay, Norway: Inter-annual variability over a 25-year time-series. Food Addit. Contam. Part A Chem. Anal. Control Expo. Risk Assess. **29**: 1605–1615. doi:10.1080/19440049.2012.714908

Nielsen, L. T., B. Krock, and P. J. Hansen. 2013. Production and excretion of okadaic acid, pectenotoxin-2 and a novel dinophysistoxin from the DSP-causing marine dinoflagellate *Dinophysis acuta* - effects of light, food availability and growth phase. Harmful Algae **23**: 34–45. doi:10.1016/j.hal.2012.12.004

O'Brien, T. D., P. H. Wiebe, and T. Falkenhaug [eds.]. 2013. ICES zooplankton status report 2010/2011. ICES Cooperative Research Report No. 318.

O'Mahony, M. 2018. EU regulatory risk management of marine biotoxins in the marine bivalve mollusc food-chain. Toxins **10**: 118. doi:10.3390/toxins10030118

Pizarro, G., B. Paz, S. González-Gil, J. M. Franco, and B. Reguera. 2009. Seasonal variability of lipophilic toxins during a *Dinophysis acuta* bloom in Western Iberia: Differences between picked cells and plankton concentrates. Harmful Algae **8**: 926–937. doi:10.1016/j.hal.2009.05.004

Pizarro, G., Á. Moroño, B. Paz, J. M. Franco, Y. Pazos, and B. Reguera. 2013. Evaluation of passive samplers as a monitoring tool for early warning of dinophysis toxins in shellfish. Mar. Drugs **11**: 3823–3845. doi:10.3390/md11103823

Prevett, A., J. Lindström, J. Xu, B. Karlson, and E. Selander. 2019. Grazer-induced bioluminescence gives dinoflagellates a competitive edge. Curr. Biol. **29**: R551–R567. doi:10.1016/j.cub.2019.05.019

R Core Team, 2019. R: A language and environment for statistical computing. R Foundation for Statistical Computing, Vienna, Austria. https://www.R-project.org/.

Reguera, B., P. Riobó, F. Rodríguez, P. A. Díaz, G. Pizarro, B. Paz, J. M. Franco, and J. Blanco. 2014. Dinophysis toxins: Causative organisms, distribution and fate in shellfish. Mar. Drugs **12**: 394–461. doi:10.3390/md12010394

Rehnstam-Holm, A. S., and B. Hernroth. 2005. Shellfish and public health: A Swedish perspective. Ambio **34**: 139–144. doi:10.1579/0044-7447-34.2.139

Roué, M., H. T. Darius, and M. Chinain. 2018. Solid Phase Adsorption Toxin Tracking (SPATT) technology for the monitoring of aquatic toxins: A review. Toxins **10**: 167. doi:10.3390/toxins10040167

Sampayo, M. A., P. Alvito, S. Franca, and I. Spusa. 1990. *Dinophysis* spp. toxicity and relation to accompanying species, p. 215–220. *In* E. Granéli, B. Sundström, L. Edler, and D. M. Anderson [eds.], Toxic marine phytoplankton. Elsevier. New York, NY, USA.

Seeyave, S., T. A. Probyn, G. C. Pitcher, M. I. Lucas, and D. A. Purdie. 2009. Nitrogen nutrition in assemblages dominated by *Pseudo-nitzschia* spp., *Alexandrium catenella* and

Dinophysis acuminata off the west coast of South Africa. Mar. Ecol. Prog. Ser. **379**: 91–107. doi:10.3354/meps07898

Selander, E., P. Thor, G. Toth, and H. Pavia. 2006. Copepods induce paralytic shellfish toxin production in marine dinoflagellates. Proc. Biol. Sci. **273**: 1673–1680. doi:10.1098/rspb.2006.3502

Selander, E., T. Fagerberg, S. Wohlra, and H. Paviae. 2012. Fight and flight in dinoflagellates? Kinetics of simultaneous grazer-induced responses in *Alexandrium tamarense*. Limnol. Oceanogr. **57**: 58–64. doi:10.4319/lo.2012.57.1.0058

Selander, E., J. Kubanek, M. Hamberg, M. X. Andersson, G. Cervin, and H. Pavia. 2015. Predator lipids induce paralytic shellfish toxins in bloom-forming algae. Proc. Natl. Acad. Sci. USA **112**: 6395–6400. doi:10.1073/pnas.1420154112

Selander, E., and others. 2019. Copepods drive large-scale trait-mediated effects in marine plankton. Sci. Adv. **5**: 3–9. doi:10.1126/sciadv.aat5096

Seltenrich, N. 2014. Keeping tabs on habs. Environ. Health Perspect. **122**: A207–A213. doi:10.1289/ehp.122-A206

Senft-Batoh, C. D., H. G. Dam, S. E. Shumway, G. H. Wikfors, and C. D. Schlichting. 2015. Influence of predator–prey evolutionary history, chemical alarm-cues, and feeding selection on induction of toxin production in a marine dinoflagellate. Limnol. Oceanogr. **60**: 318–328. doi:10.1111/lno.10027

Smayda, T. J. 2008. Complexity in the eutrophication-harmful algal bloom relationship, with comment on the importance of grazing. Harmful Algae **8**: 140–151. doi:10.1016/j.hal.2008.08.018

Smith, J. L., M. Tong, D. Kulis, and D. M. Anderson. 2018. Effect of ciliate strain, size, and nutritional content on the growth and toxicity of mixotrophic *Dinophysis acuminata*. Harmful Algae **78**: 95–105. doi:10.1016/j.hal.2018.08.001

Spanbauer, T. L., C. Briseño-Avena, K. J. Pitz, and E. Suter. 2020. Salty sensors, fresh ideas: The use of molecular and imaging sensors in understanding plankton dynamics across marine and freshwater ecosystems. Limnol. Oceanogr.: Lett. **5**: 169–184. doi:10.1002/lol2.10128

Sundh, U. B., and J. Toljander. 2017. Mikrobiologiska och kemiska risker med musslor och ostron innehåll. Livsmedelsverket National Food Agency, Uppsala, Sweden. 20. https://www.livsmedelsverket.se/globalassets/publikationsdatabas/rapporter/2017/riskvarderingsrapport-mikrobiologiska-och-kemiska-risker-med-musslor-och-ostron-livsmedelsverkets-rapportserie-20-2017-del-2.pdf

Suzuki, T., and others. 2012. LC-MS/MS analysis of novel ovatoxin isomers in several *Ostreopsis* strains collected in Japan. Harmful Algae **20**: 81–91. doi:10.1016/j.hal.2012.08.002

Swan, S. C., A. D. Turner, E. Bresnan, C. Whyte, R. F. Paterson, S. McNeill, E. Mitchell, and K. Davidson. 2018. *Dinophysis acuta* in Scottish coastal waters and its influence on diarrhetic shellfish toxin profiles. Toxins **10**: 399. doi:10.3390/toxins10100399

Teegarden, G. J. 1999. Copepod grazing selection and particle discrimination on the basis of PSP toxin content. Mar. Ecol. Prog. Ser. **181**: 163–176. doi:10.3354/meps181163

Teegarden, G. J., R. G. Campbell, and E. G. Durbin. 2001. Zooplankton feeding behavior and particle selection in natural plankton assemblages containing toxic *Alexandrium* spp. Mar. Ecol. Prog. Ser. **218**: 213–226. doi:10.3354/meps218213

Tillmann, U., D. Jaén, L. Fernández, M. Gottschling, M. Witt, J. Blanco, and B. Krock. 2017. *Amphidoma languida* (Amphidomatacea, Dinophyceae) with a novel azaspiracid toxin profile identified as the cause of molluscan contamination at the Atlantic coast of southern Spain. Harmful Algae **62**: 113–126. doi:10.1016/j.hal.2016.12.001

Tong, M., D. M. Kulis, E. Fux, J. L. Smith, P. Hess, Q. Zhou, and D. M. Anderson. 2011. The effects of growth phase and light intensity on toxin production by *Dinophysis acuminata* from the northeastern United States. Harmful Algae **10**: 254–264. doi:10.1016/j.hal.2010.10.005

Turner, A. D., and others. 2011. Comparison of AOAC 2005.06 LC official method with other methodologies for the quantitation of paralytic shellfish poisoning toxins in UK shellfish species. Anal. Bioanal. Chem. **399**: 1257–1270. doi:10.1007/s00216-010-4428-7

Turner, A. D., and others. 2012. Investigations into matrix components affecting the performance of the official bioassay reference method for quantitation of paralytic shellfish poisoning toxins in oysters. Toxicon **59**: 215–230. doi:10.1016/j.toxicon.2011.11.013

Turner, J. T. 2014. Planktonic marine copepods and harmful algae. Harmful Algae **32**: 81–93. doi:10.1016/j.hal.2013.12.001

Turner, J. T., and P. A. Tester. 1997. Toxic marine phytoplankton, zooplankton grazers, and pelagic food webs. Limnol. Oceanogr. **42**: 1203–1213. doi:10.4319/lo.1997.42.5_part_2.1203

Turner, J. T., and D. G. Borkman. 2005. Impact of zooplankton grazing on *Alexandrium* blooms in the offshore Gulf of Maine. Deep-Sea Res. II Top. Stud. Oceanogr. **52**: 2801–2816. doi:10.1016/j.dsr2.2005.06.011

Turrell, E. A., and L. Stobo. 2007. A comparison of the mouse bioassay with liquid chromatography-mass spectrometry for the detection of lipophilic toxins in shellfish from Scottish waters. Toxicon **50**: 442–447. doi:10.1016/j.toxicon.2007.04.002

Wexels Riser, C., S. Jansen, U. Bathmann, and P. Wassmann. 2003. Grazing of *Calanus helgolandicus* on *Dinophysis norvegica* during bloom conditions in the North Sea: Evidence from investigations of faecal pellets. Mar. Ecol. Prog. Ser. **256**: 301–304. doi:10.3354/meps256301

Wood, S. N. 2011. Fast stable restricted maximum likelihood and marginal likelihood estimation of semiparametric generalized linear models. J. R. Stat. Soc. Series B Stat. Methodol. **73**: 3–36. doi:10.1111/j.1467-9868.2010.00749.x

Xu, J., and T. Kiørboe. 2018. Toxic dinoflagellates produce true grazer deterrents. Ecology **99**: 2240–2249. doi:10.1002/ecy.2479

Zhang, H., W. Hu, K. Gu, Q. Li, D. Zheng, and S. Zhai. 2013. An improved ecological model and software for short-term algal bloom forecasting. Environ. Model. Softw. **48**: 152–162. doi:10.1016/j.envsoft.2013.07.001

Acknowledgments

We would like to acknowledge Malin Persson and Jonas Renhult at the Swedish Food Agency for providing shellfish samples and Bengt Karlson for assistance with *Dinophysis* data. We would also like to thank Kristie Rigby, Andrew Prevett, and Wiebke Grebner for technical assistance. This project was funded by a grant to ES from the Swedish Research Council VR, 2019-05238.

Conflict of Interest

None declared.

Submitted 03 November 2020
Revised 02 March 2021
Accepted 27 June 2021

Associate editor: Birte Matthiessen